



3D Engineered Fiberboard: Engineering Analysis of a New Building Product

John F. Hunt and Jerrold E. Winandy

USDA Forest Service, Forest Products Laboratory,

Madison, WI 53726 USA

ABSTRACT: In many forests across the United States, the high forest fuel loadings are contributing to our recent forest fire problems. Many fire-prone timber stands are generally far from traditional timber markets or the timber is not economically valuable enough to cover the costs of removal. To help address this problem, the USDA Forest Products Laboratory has developed a process to produce three-dimensional structural fiberboard products that can utilize the wide range of lignocellulosic fibers contained in the forest undergrowth, underutilized timber, and agro-biomass. In this way, removing these components of the forest can be encouraged by the private sector, dangerous fuels can thereby be removed, and costs to the federal government for fire mitigation can be minimized.

The newly developed product consists of an engineered wet-pulp-molded structural material molded into an engineered form by forming and hot-pressing the fibers between rigid molds with or without supplemental adhesive. This hot pressing produces strong inter-fiber bonds even when using relatively low-quality fiber. When the structural core is bonded to exterior skins, three-dimensional sandwich panels, called '3D Engineered Fiberboard' are formed that exhibits a high level of strength and stiffness with significantly less material. Preliminary 3D engineering analyses are presented. The proposed technology has a number of promising uses in construction, furniture and packaging applications. The economic feasibility of constructing panels from these materials is also currently being assessed as part of our on-going research program

KEYWORDS: 3D structures, engineered fiberboard, engineering analysis, wood fiber

INTRODUCTION

Currently, after logging or thinning operations much of the low value timber is either left standing or is felled and left on the ground, chipped, or burned because most North American mills are not equipped to handle this material. In many areas of Western U.S., this forest residue does not decompose if felled and it soon becomes susceptible to forest insect or disease if partially damaged or injured during logging and an increasing fire hazard as it dries.

Two research projects are currently in their second year of a three-year project funded under the USDA Forest Service "National Fire Plan" [1, 2]. The goal of these two research projects is to maintain a healthy and sustainable forests through development of economically viable process(es) and product(s) that can utilize small-diameter timber, forest undergrowth, and whole tree trimmings from logging operations. In this way, "whole-site" forest management can be implemented to use all available living biomass material for optimum utilization leaving minimal impact in the forest for future insect, disease, or forest fire damage. By providing economical options for all these materials this can then reduce costs to the federal government for improved forest health, eco-system and minimized fire mitigation and also encourage rural development.

The overall goal of each research project is to help maintain a healthy and sustainable forest by developing uses for whole-tree material from underutilized trees, logging residuals, and forest undergrowth to produce value-added materials such as three-dimensional (3D) engineered structural fiberboard. This paper briefly describes the fiber processing used in this study and focuses on the engineering analysis needed to develop a value-added 3D engineered structural fiberboard.

BACKGROUND

When a lightweight three-dimensional (3D) structural core material (Fig.1) is bonded between two flat panels, a three-dimensional sandwich panel is formed that exhibits high strength and stiffness to weight ratio. The USDA Forest Products Laboratory has been working on methods to process various types of lignocellulosic fibers into bondable fibrous mixtures that can be formed into 3D structures and then dried in a prescribed way to achieve a 3D engineered fiberboard with predictable performance properties. This project uses low-value materials currently being left in the forest; developing a low-cost method to process the material into a bondable fibrous material; and forming and hot-pressing those fibers into a value-added 3D structural product. The proposed technology has promising uses in the construction of pallets, bulk bins, heavy duty boxes, shipping containers, packaging supports, wall panels, roof panels, cement forms, partitions, displays, reels, desks, caskets, shelves, tables, and doors. The size of these potential markets is enormous. For example, according to 1996 statistics published in the Annual Survey of Manufacturers, the pallet industry has annual sales in the U.S. of over \$3 billion, wood office furniture is a \$2.4 billion market, wood partitions and fixtures are a \$3.7 billion market, and wood doors account for \$2.2 billion of the total door market.



Fig.1 preliminary design of a uniaxial core made from fiberized fibers from small diameter tree tops

EXPERIMENTAL

Material Selection and Fabrication: The fibrous material used for this study was obtained from small diameter treetops less than 10 cm (4 in) diameter as part of a USDA National Fire Plan Project [1]. They were fiberized with the bark using existing industrial fiberizing technology from Bolton-Emerson Inc. [3] and atmospheric refining at the Forest Products Laboratory. The material would then be wet-formed and press-dried into 3D engineered fiberboard panels. We investigated nineteen potential fiberizing methods to determine their effects on basic material properties. After each fiberization run, the fibers were made into flat panels 2.5 mm (0.1 in) thick. The fibers bonded together under heat and pressure without adhesives or additives. The flat panels were evaluated for their physical and mechanical properties following American Society for Testing and Materials Standard D-1037 [4] methods. For the engineering analysis part of this study, we used the material properties from runs 18 and 30 (Table 1) representing the low and high properties from the processing options. The fiberizing processes are described in more detail in a paper presented at the 6th European Panel Products Symposium [5].

Table 1 Tensile modulus of elasticity (MOE) and tensile strength properties for flat panels made from small diameter trees.

Run No.	Panel Forming Conditions	Tensile MOE	Tensile Strength
Rm 18	0% NaOH, 90°C	5.6 GPa (0.82 MPa)	41 MPa (5955 PSI)
Rm 30	4% NaOH, 90°C	6.1 GPa (0.89 MPa)	44 MPa (6416 PSI)

Engineering Analysis: An engineering analysis was conducted to determine the potential performance of a 3D engineered fiberboard product with uniaxial ribs aligned down the length of the panel (Fig. 1 and Fig. 2). A fixed total panel thickness of 38.1 mm (1.5 in) and face thickness of 4.76 mm (0.1875 in) were chosen as starting points for this initial analysis. A 3x3x3 experimental design matrix (Table 2) was used where factor 1 was the repeated pattern width 50.8, 76.2, 101.6 mm (2, 3, and 4 inch) (Table 3); factor 2 was the rib angle 90, 70, and 50 degrees; and factor 3 was the rib wall thickness 1.27, 1.90, and 2.54 mm (0.05, 0.075, and 0.1 inch).

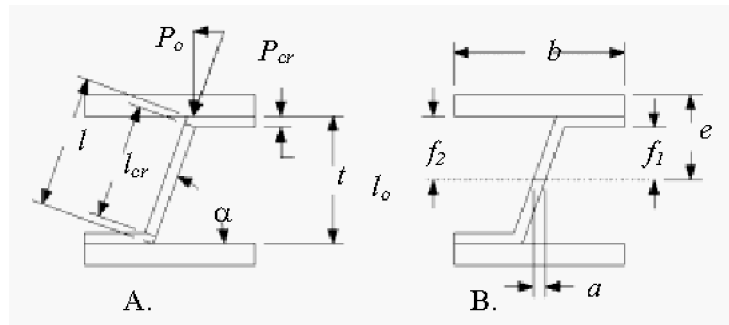


Fig. 2 (A) Geometry, considerations for determining normal load, P_o , per rib per unit depth for both compression and buckling failure mechanism; (B) variables used to describe the geometry, to estimate shear stress.

Table 2 Study 3x3x3 design matrix for the engineering analysis.

3x3x3 design matrix		Pattern Width		
		50.8 mm (2.0 in)	76.2 mm (3.0 in)	101.6 mm (4.0 in)
Rib Angle	90 degrees	<u>Rib Thickness</u> 1.27 mm (0.05 in)	<u>Rib Thickness</u> 1.27 mm (0.05 in)	<u>Rib Thickness</u> 1.27 mm (0.05 in)
		1.90 mm (0.075 in)	1.90 mm (0.075 in)	1.90 mm (0.075 in)
		2.54 mm (0.1 in)	2.54 mm (0.1 in)	2.54 mm (0.1 in)
	70 degrees	<u>Rib Thickness</u> 1.27 mm (0.05 in)	<u>Rib Thickness</u> 1.27 mm (0.05 in)	<u>Rib Thickness</u> 1.27 mm (0.05 in)
		1.90 mm (0.075 in)	1.90 mm (0.075 in)	1.90 mm (0.075 in)
		2.54 mm (0.1 in)	2.54 mm (0.1 in)	2.54 mm (0.1 in)
	50 degrees	<u>Rib Thickness</u> 1.27 mm (0.05 in)	<u>Rib Thickness</u> 1.27 mm (0.05 in)	<u>Rib Thickness</u> 1.27 mm (0.05 in)
		1.90 mm (0.075 in)	1.90 mm (0.075 in)	1.90 mm (0.075 in)
		2.54 mm (0.1 in)	2.54 mm (0.1 in)	2.54 mm (0.1 in)

Table 3 Three pattern widths (factor 1) used for this study are expanded here across a 15.2 cm (6.0 in) panel width for clarity of the drawings.

50.8 mm (2.0 in) Pattern Width with 90 degree rib angle shown repeated 3 times.	
76.2 mm (3.0 in) Pattern Width with 90 degree rib angle shown repeated 2 times	
101.6 mm (4.0 in) Pattern Width with 90 degree rib angle shown repeated 1.5 times	

Bending: Mid-point loading equation for beam deflection is shown in Equation 1. Deformation was calculated and plotted (Fig. 3) for each of the configurations at the same load per unit width 8.75 kN/m (50 lb/in). The mid-point load for each pattern width can be calculated by multiplying the load times the beam width. To achieve equal comparison, the pattern widths were expanded to equal beam widths, as shown in Table 3. The tension MOE values (Table 1) obtained from the mechanical test were used to estimate deformation.

$$y = \frac{-P_o L^3}{48EI_b} \tag{1}$$

Where y is beam deflection; P_o is the beam load; L is total span length, $L = 0.91$ m (36 in); E is the longitudinal tensile modulus of elasticity; I_b is the area moment of inertia for the combined beam cross-section.

Beam deflections for all rib angles, rib thickness', and both MOEs are plotted for each pattern width. (Figure 3). It can be seen there is little difference between the calculated deformation values for all the different corrugated configurations. This is because the I_b for the faces represent 85 to 95% of the total, so small variations in the corrugated geometry do not have a significant impact on the total I_b and hence the total deformation. However, comparing the deformation of the engineered fiberboard with particleboard shows the engineered fiberboard's stiffness is significantly higher (lower beam deflection) than that of an equivalent dimensioned medium or high density particleboard beam. The engineered fiberboard's cross-sectional area is reduced by approximately 2/3rd compared to a solid particleboard beam. This is significant material savings while surpassing the performance of particleboard.

Calculating bending deflections perpendicular to the rib alignment is difficult since there is not a uniform cross-section that we could use to determine the area moment of inertia. For this bending arrangement we would use the I for the faces only. The resulting deflection or load calculations would represent conservative values. We will analyze this bending situation in more detail in a later publication.

Failure in bending could occur in tension or compression failure of the faces or as shear failure in the core. Equation 2 rearranges the terms in the modulus of rupture calculation so we can determine an estimated load (P_o) for failure to occur in the faces. For our estimates we are assuming the maximum tension and compression stress (\mathbf{s}_{cr}) are the same. Calculating shear stress in a sandwich panel is a little difficult especially if the geometry is slightly non-uniform as is our corrugated structure. Marks' Handbook [6] provides an equation to determine shear stress for an I-beam. Again rearranging the terms to calculate an estimated load (P_o) for shear failure is shown in Equation 3. Maximum shear stress (\mathbf{l}_{cr}) is assumed to be 1/2 the maximum tension stress for a first approximation. This is obtained using Mohr's circle for equal compression and tension stress. Because our geometry is not exactly an I-Beam, it is assumed the term f is the average value of f_1 and f_2 (Fig. 2B).

$$P_o = \frac{I_b \sigma_{cr}}{(L/2)y} \tag{2}$$

Where L is the total span length and y is the distance from the neutral axis to the outer dimension

$$P_o = \frac{\tau_{cr} 4a}{3} \left[\frac{be^3 - (b-a)f^3}{be^2 - (b-a)f^2} \right] \quad 3$$

Where a , b , e , and f are dimensions defined in Fig. 2B.

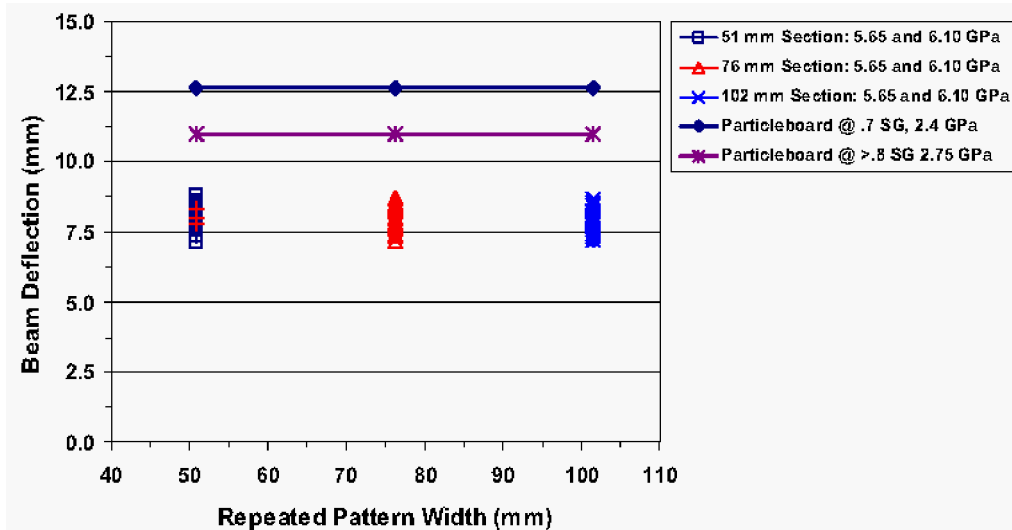


Fig. 3 beam deflection for the engineered fiberboard shape compared with particleboard Deflection data for all Configurations are plotted; three rib angles, three rib thicknesses and both MOEs are shown grouped together according to the three pattern widths.

Flat Crush: While bending deflection data provides engineers with performance characteristics for many applications, there are many other applications where load carrying normal to the panel is needed. When using solid panel products there is not much concern for compression failure because the solid structure does not exhibit crushing for most applications. However, for a 3D engineered fiberboard where material has been removed from the core for engineering and material efficiency, compression loads must be considered. For a ribbed structure, two possible modes of failure are possible when loading normal to the panel: compression and buckling failure. Depending on the geometry and elastic properties, one or the other failure mechanisms may occur before the other. For compression, failure criteria is based only on the maximum compressive stress (s_{cr}) properties parallel to the rib. Using an estimated maximum compressive stress value ($s_{cr} = 41$ or 44 MPa) for the material in the ribs, as described in the Section 3.2.3, it is possible to solve for an estimated maximum load carrying (P_{cr-c}) capacity per rib per unit depth (Eq. 4). As the rib angle (α) decreases, the normal load (P_o) (Eq. 5 and Fig. 2) decreases or in other words the panel load carrying capacity decreases as the rib angle decreases.

$$P_{cr-c} = \sigma_{cr}(t*1) \quad 4$$

Where t is rib thickness and 1 is the unit depth.

$$P_o = P_{cr} \cos(90 - \alpha) \quad 5$$

Compression failure criteria does not take into consideration any geometry issues of the ribs. If the rib length:thickness ($l_{cr}:t$) ratio is too high, then the ribs can act as miniature columns and fail by buckling far below the calculated compression failure stress. Equation 6 is used to estimate the critical load (P_{cr-b}) when buckling failure would occur.

$$P_{cr-b} = \frac{n \pi^2 EI_r}{l_{cr}^2} \quad 6$$

Where n is the column end condition factor, $n = 2$ for both ends fixed [5], E is the modulus of elasticity, I_r is the area moment of inertia for the ribs' cross-section, and l_{cr} is the rib column length (Fig. 2A).

For this analysis, we selected a ($l_{cr}:t$) ratio that fell between the two failure mechanisms of buckling and compression failure. In Fig. 4, buckling vs. compression failure loads are plotted for ribs at 1.27, 1.90, and 2.54 mm and rib angles at 50, 70, and 90 degrees for a material having an MOE of 5.6 GPa (Run 18 material properties). The solid lines are estimated buckling failure loads and dashed lines are estimated compression failure loads. Failure will occur at the lower value of either the buckling or compression load. For the thinnest rib (1.27 mm) it shows failure will always occur due to buckling for all rib angles. For the 1.90 mm thick rib, buckling will occur at rib angles below 65 degrees and rib compression will occur above 65 degrees. The 2.54 mm thick rib is estimated to fail in compression for all the angles before ever reaching the buckling load.

Another engineering assessment for design is determining if flat-wise deformation is within acceptable limits. Using the MOE equation relationship of stress/strain, the basic terms can be rearranged to determine the change in thickness normal to the faces (Δl_o) (Fig. 2) due to compressive loads using Eq. (7).

$$\Delta l_o = \frac{l_o P_{cr}}{t * 1} \quad 7$$

Where l_o is the original core rib height.

Prior to calculating the change in total thickness, it is important to have determined the failure mode, buckling or compression, and the appropriate P_{cr} . In Fig.5, panel deformation is plotted per rib per unit depth. It shows the effects of rib angle, rib thickness, MOE, type of failure, and normal load on panel deformation. Normal load carrying capacity significantly decreases as rib angle and thickness decreases (Fig. 5). This is important to remember when balancing the performance requirements with practical fiber forming characteristics and pressing methods. A reduced angle may be necessary for optimum fiber processing, which may then require a thicker rib or stiffer material to achieve the desired load carrying performance needs. Depending on the design, a thicker rib or stiffer material may change the failure mechanism from buckling to compression allowing the rib to carry even higher loads.

So far we have only considered the load per rib per unit depth. The number of ribs per unit width of the panel will also change load-carrying performance. This is a linear relationship where doubling or triple the ribs per unit width will double or triple the normal load carrying capability or reduce by half or a third the deformation at a given load. The number of ribs per unit width has a practical upper limit based on fiber forming characteristics. Also, 90 degree ribs, while easy to describe geometrically and calculate the loads based on the angles, it is difficult to apply the necessary consolidation forces normal to the fiber rib geometry during hot press-drying. As the rib angle decreases, it is easier to consolidate the ribs using a conventional hydraulic hot-press and forming molds. The maximum number of ribs and the angles for optimum consolidation are sufficiently difficult to describe and would require additional definitions, which is outside the scope of this paper. These and other forming considerations will be developed in a later publication.

Engineering Assumptions: For this analysis it is assumed that the material properties are isotropic and linear elastic. We did not test the material in compression but assumed compression strengths were equal to the tensile strength. This assumption is based on similar tension-to-compression strength comparisons for wet-formed hardboard [7]. Flat crush deformation (per unit depth) assumes no buckling has taken place in the rib.

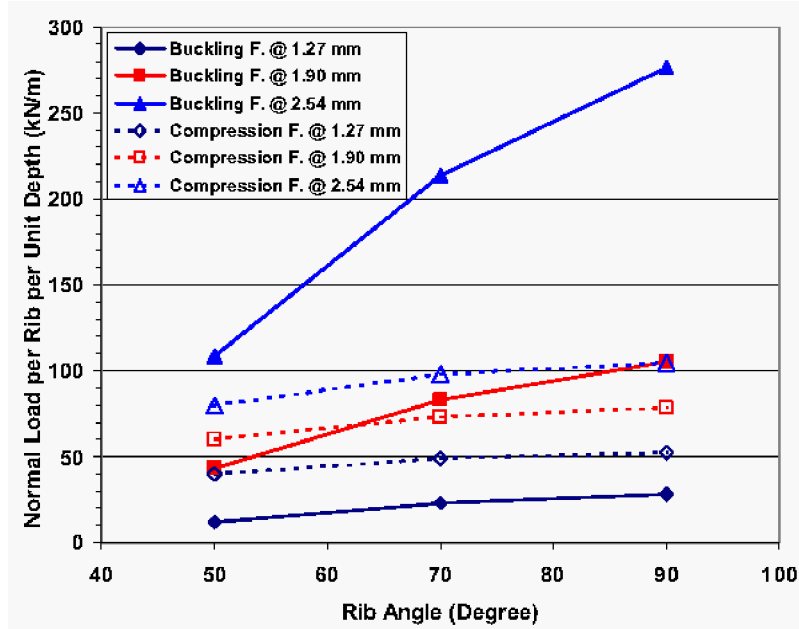


Fig. 4 comparison of normal load per rib per unit depth for buckling vs. compression failure mechanisms. Failure occurs at the lower value of either the buckling or compression values for a given rib thickness. (Ribs at 1.27 mm all fail in buckling while the ribs for 1.90 mm will fail in compression at 65 degrees and greater.)

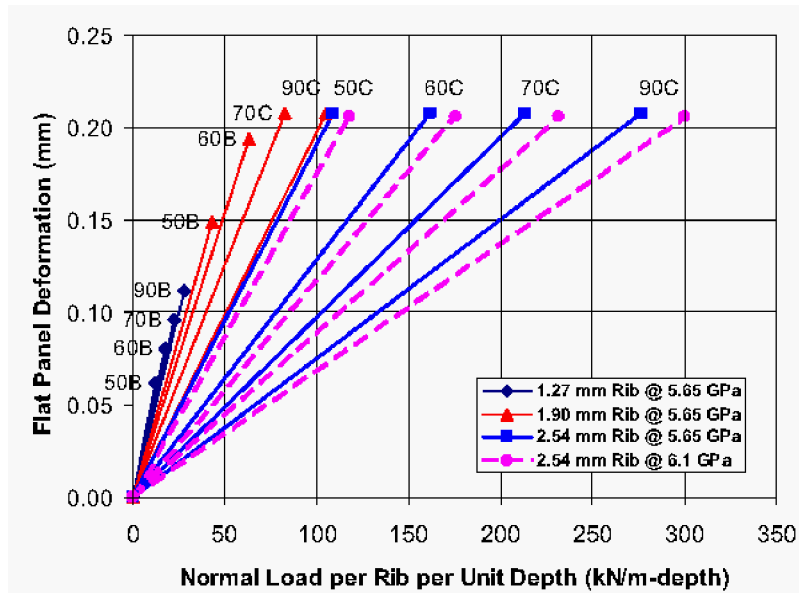


Fig. 5 Panel deformation as a function of rib thickness for MOE = 5.65 and 6.10 GPa. Letters at rib degrees indicate failure mode. (B = Buckling, C = Compression)

SUMMARY

Based on the mechanical properties of flat panels produced from the fiberized small diameter material and through this engineering analysis, it can be shown that a 3D engineered fiberboard could be designed to be stiffer than minimum particleboard standards with approximately 2/3rd less material. The analysis also shows the performance properties can be manipulated depending on the rib pattern width, rib angle, rib thickness, and material properties. If low-valued materials were used to fabricate

a value-added engineered product it possibly could compete in existing markets. If the fiberizing and 3D processing economics prove favorable, a 3D engineered product may provide sufficient economic incentive for the private sector to develop engineered products in rural areas new the fiber resources. While in this study we used material properties from panels that did not use my adhesives to bond the fibers together, performance characteristics could be improved with traditional fiber resins or additives.

The analysis provides simplified equations for estimating bending and flat crush performance characteristics for a simple corrugated sandwich panel while being aware of multiple failure modes.

Further research will verify these equations and assumptions when full panels are tested. An economic feasibility of constructing panels from these materials using these processes is also being conducted at the Forest Products Laboratory.

REFERENCES

1. Hunt, J.F. 2000. "*Hazardous fuels reduction through harvesting underutilized trees and forest undergrowth and producing three-dimensional structural products.*" USDA Forest Service, Forest Products Laboratory Proposal No. 01.FPL.C.1 to USDA Forest Service, National Fire Plan.
2. Hunt, J.F. 2000. "*Utilization of small diameter crooked timber for use in laminated structural boards through development of new sawing, laminating, and drying processes.*" USDA Forest Service, Forest Products Laboratory Proposal No. 01.FPL.C.2 to USDA Forest Service, National Fire Plan.
3. BOLTON-EMERSON INC. "*The Tornado Pulper*" Bolton-Emerson Americas, Inc.: Lawrence, MA, USA
4. ASTM Standard "*D 1037 (1996): Evaluating the Properties of Wood-Base Fiber and Particle Panel Materials*". American Society for Testing and Materials, West Conshohocken, PA
5. Hunt, J.F. and Winandy, J.E.. 2002. "*3D Engineered Fiberboard: A New Structural Building Product*", 6th European Panel Products Symposium. Oct. 9-11, 2002. Llandudno, Wales. pp106-117
6. Avallone, E.A. and Baumeister III, T.. 1987. "*Mark's Standard Handbook of Mechanical Engineering 9th Edition*", McGRAW-HILL, INC., New York.
7. Suchsland, O. and Woodson, G.E.. 1986. "*Fiberboard Manufacturing Practices in the United States*". USDA Forest Service, Agriculture Handbook No. 640.